Crystal Structure of the Mammalian Grb2 Adaptor

Sébastien Maignan, Jean-Pierre Guilloteau, Nadine Fromage, Bernadette Arnoux, Jérôme Becquart, Arnaud Ducruix*

The mammalian growth factor receptor–binding protein Grb2 is an adaptor that mediates activation of guanine nucleotide exchange on Ras. Grb2 binds to the receptor through its SH2 domain and to the carboxyl-terminal domain of Son of sevenless through its two SH3 domains. It is thus a key element in the signal transduction pathway. The crystal structure of Grb2 was determined to 3.1 angstrom resolution. The asymmetric unit is composed of an embedded dimer. The interlaced junctions between the SH2 and SH3 domains bring the two adjacent faces of the SH3 domains in van der Waals contact but leave room for the binding of proline-rich peptides.

The 25-kD adaptor protein Grb2 is the human homolog (*1*) of Sem-5 protein from *Caenorhabditis elegans* (*2*) and of Drk from *Drosophila melanogaster* (*3*). It is a modular protein composed of one SH2 and two SH3 domains (*4*). After activation and phosphorylation of the epidermal growth factor (EGF) receptor, the Grb2-Sos complex is recruited to the membrane in an SH2-dependent manner and activates the Ras signaling pathway. Recently it has been suggested that regulation of Grb2 may play a role in apoptosis (*5*). The SH2 domain of Grb2 also binds to class II phosphotyrosyl peptides with consensus sequence pYXNX with a preference for residues Q, Y, and V at position +1 and Y, Q, and F at position +3 relative to the phosphotyrosine (*6*, *7*).

The SH3 domain of Grb2 binds to Sos and Sos-derived, proline-rich peptides (*8*). SH3 domains can bind peptides in two opposite orientations (plus and minus) (*9*). Solution structures of Grb2 NH_2-terminal (*10*) and COOH-terminal (*11*) SH3 domains with bound peptides were recently determined. They show that Grb2 binds PPPVPPRRR peptides in the minus orientation as previously postulated.

Crystals were obtained at 19°C by dialysis from a Grb2 solution (15 mg/ml) with sodium acetate (pH 8.0) as a crystallizing agent. They belong to space group $P4_3$ with $a = b = 90.0$ Å and $c = 97.7$ Å and contain two molecules in the asymmetric unit (*12*). The crystal structure of Grb2 (Fig. 1) shows three distinct domains. Within a molecule of Grb2, the SH3 domains are not in contact with the SH2 domain. They are separated by an interlaced junction with few contacts that resembles a pair of suspenders. The crystal structure indicates that the relative positions of the three domains in the protein leave the three binding sites fully accessible. This makes it very unlikely that a conformational change in the Grb2 SH2 domain could be transmitted to the Sos proline-rich binding sites of SH3 domains and vice versa.

Each SH3 domain forms a β barrel, as previously described in other x-ray or nuclear magnetic resonance structures (*9*, *13*). It consists of five antiparallel stranded β sheets. The two SH3 domains have 36% sequence identity and Cα can be superimposed within 1.35 Å root mean square. Much attention has focused on the binding of peptides to Grb2 SH3 domains (*9*–*11*). Some bind preferentially to the NH_2-terminal domain, others to the COOH-terminal one. At both sites, the peptide backbone adopts a polyproline type II helix conformation in the minus orientation. As shown in Fig. 2, the binding regions of the two SH3 domains are ~34 Å apart. Because of their proximity, the two SH3 domains form a continuous surface at the bottom of the molecule, which presents an alignment of negatively charged residues. This arrangement clearly favors a tighter binding of peptides with basic residues, Both SH3 domains of Grb2 contain an RGD sequence that forms a quite accessible turn.

The interface between the two SH3 domains is mainly defined by van der Waals contacts and buries only 1000 $Å^2$ with 5 hydrogen bonds as compared to a typical (*14*) protein-protein interface of 1500 Å containing 10 hydrogen bonds. Due to the small area of this interface, it is possible that the two SH3 domains of Grb2 could dissociate and adopt different orientations (Fig. 3), allowing Grb2 to be a flexible adaptor. The relative position of the Lck SH2-SH3 domains (*15*) (Lck is a member of the Src-family tyrosine kinases) is different. When 'the SH2 domains are superimposed (Fig. 4), the SH3 domain of Lck is 90° away from those of Grb2. These observations support an independent function of SH2 and SH3 domains in such modular proteins.

The SH2 domain of Grb2, which recognizes phosphorylated peptides, is made of a

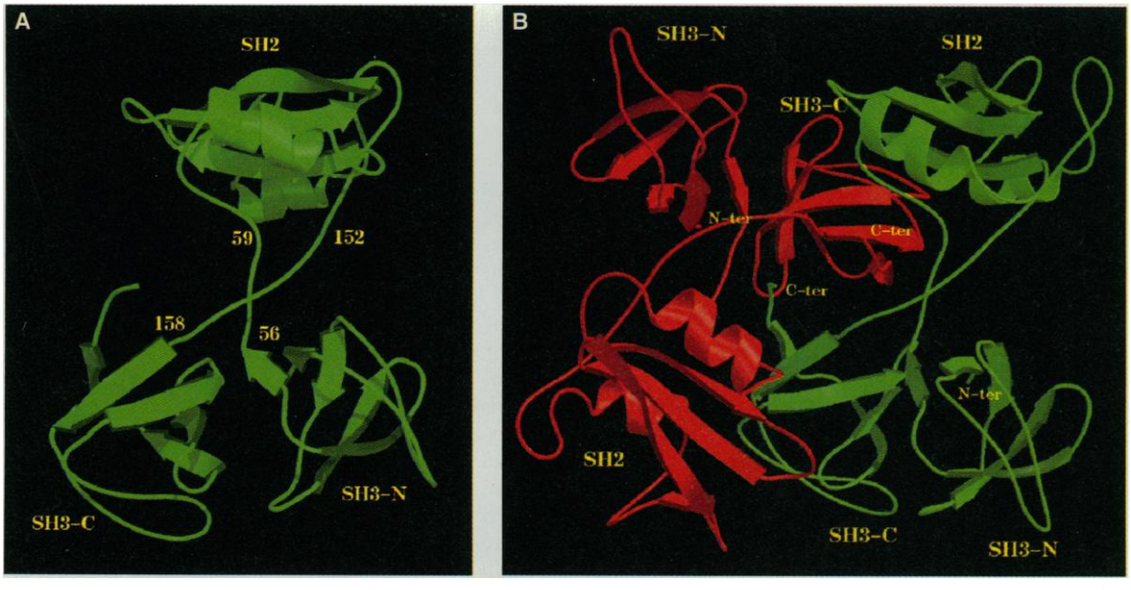

Fig. 1. (**A**) Ribbon diagram of Grb2 produced with the program Molscript (*22*) and Raster3D (*23*). (**B**) Ribbon diagram of the dimer of Grb2. Molecule A is colored in green and molecule B in red.

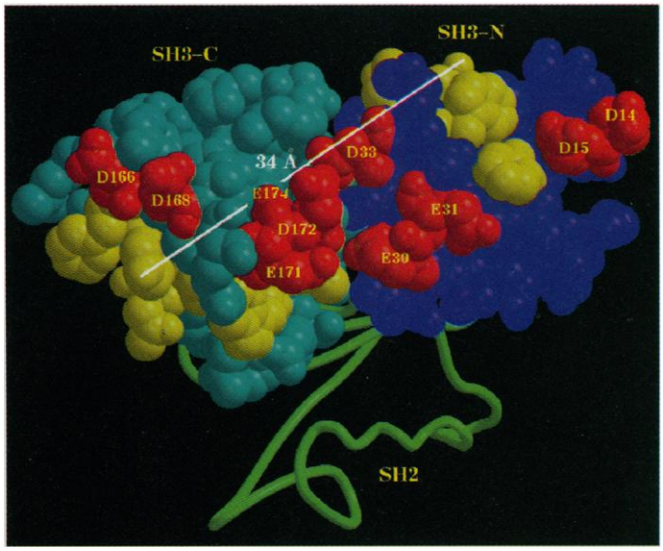

Fig. 2. Space-filling model of the SH3 domain binding sites. The ribbon diagram of the SH2 domain is colored in green, the NH_2-terminal SH3 in dark blue, the COOH-terminal SH3 in light blue, and the peptide binding sites are in yellow. The row of negatively charged residues Asp^{14}, Asp^{15}, Glu^{30}, Glu^{31}, Asp^{33}, Asp^{166}, Asp^{168}, Glu^{171}, Asp^{172}, and Glu^{174} is colored in red.

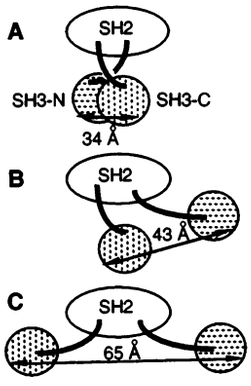

Fig. 3. Schematic representation of the possible relative orientation of the SH3 domains of Grb2. N, NH_2-terminal, and C, COOH-terminal. The arrow indicates the distance between the SH3 peptide binding sites. (**A**) Closed; as observed in the Grb2 x-ray structure. (**B**) Half open. (**C**) Open.

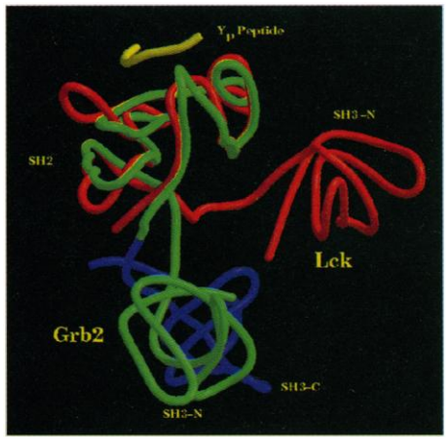

Fig. 4. Superposition of the SH2 domains of Grb2 (seen 90° from Fig. 1) with the SH2 of the Lck SH2-SH3 peptide complex in red (*15*). The associated peptide is colored in yellow. The SH2 and NH_2-terminal SH3 domains of Grb2 are in green, whereas the COOH-terminal is in dark blue.

classical (*16*, *17*) central antiparallel β sheet flanked by two helices. Grb2 binds the peptide SPGEpYVNIEFGS of insulin receptor substrate 1, where pY corresponds to Tyr^{895}. The crystal structures of this peptide complexed with the Syp tyrosine phosphatase SH2 domain, as well as of the uncomplexed Syp, have been described (*16*). Superposition of the SH2 domains of the peptide-Syp complex and of Grb2 shows the phosphorylated tyrosine of the peptide in proximity of Arg^{86} of Grb2 in agreement with binding and mutation studies, which show that this residue is a key element for peptide binding. The Grb2 jaw, made from loops EF and BG, is in a more open conformation than in other SH2 domain structures not complexed with a peptide. However, the modeling shows that Trp^{121} of Grb2 would prevent binding of the peptide due to steric hindrance with I+3 and F+5. This observation indicates that either Grb2 or the peptide should change its conformation, which is in agreement with results from fluorescence studies (*18*).

The two molecules of the asymmetric unit are related by a local twofold axis (Fig. 1B). They are embedded with the COOH-terminal extremity of molecule A sandwiched between the SH2 and COOH-terminal SH3 of molecule B and vice versa. The dimer interface (area of the protein surface that is removed from contact with the solvent) is 4100 $Å^2$. This value is quite large and suggests that Grb2 could be a dimer, although light-scattering measurements show that in diluted solutions, Grb2 behaves as a monomer. If the dimer exists in solution, the two embraced molecules would still have their peptide binding sites (two for SH2 and four for SH3) accessible and therefore dimerization would not play a regulatory function. Whether or not this dimerization plays a role in the adaptor function of Grb2 remains to be shown.

S. Maignan, B. Arnoux, A. Ducruix, Laboratoire de Biologie Structurale, Unite Mixte de Recherche CNRS–Université de Paris-Sud, 91198 Gif sur Yvette Cedex, France. J.-P. Guilloteau, N. Fromage, J. Becquart, Service de Biochimie, Rhône-Poulenc Rorer, 94403 Vitry sur Seine Cedex, France.

*To whom correspondence should be addressed.

REFERENCES AND NOTES

1. E. J. Lowenstein *et al.*, *Cell* **70**, 431 (1992); K. Matuoka, F. Shibasaki, M. Shibata, T. Takenawa, *Proc. Natl. Acad. Sci. U.S.A.* **89**, 9015 (1992).
2. S. G. Clark, M. J. Stern, H. R. Horwitz, *Nature* **356**, 340 (1992).
3. J. P. Olivier *et al.*, *Cell* **73**, 179 (1993).
4. G. B. Cohen, R. Ren, D. Baltimore, *ibid.* **80**, 237 (1995).
5. I. Fath *et al.*, *Science* **264**, 971 (1994).
6. Z. Songyang *et al.*, *Cell* **72**, 767 (1993).
7. Abbreviations for the amino acid residues are as follows: A, Ala; C, Cys; D, Asp; E, Glu; F, Phe; G, Gly; H, His; I, Ile; K, Lys; L, Leu; M, Met; N, Asn; P, Pro; Q, Gln; R, Arg; S, Ser; T, Thr; V, Val; W, Trp; and Y, Tyr. pY, phosphorylated Y.
8. P. Chardin *et al.*, *Science* **260**, 1338 (1993).
9. S. Feng, J. K. Chen, H. Yu, J. A. Simon, S. L. Schreiber, *ibid.* **266**, 1241 (1994); W. A. Lim, F. M. Richards, R. O. Fox, *Nature* **372**, 375 (1994).
10. N. Goudreau *et al.*, *Nature Struct. Biol.* **1**, 898 (1994); M. Wittekind *et al.*, *Biochemistry* **33**, 13531 (1994); H. Terasawa *et al.*, *Nature Struct. Biol.* **1**, 891 (1994).
11. D. Khoda *et al.*, *Structure* **2**, 1029 (1994).
12. Details of cloning, expression, and crystallogenesis will be published elsewhere. Phase separation or twinning often hampered production of usable crystals. All data were recorded with synchrotron radiation at LURE with a wiggler beam line (λ = 0.901 Å) and MarResearch Imaging plates. Native data were collected at 3.1 Å resolution with one crystal at 4°C. Data were processed with Mosflm. Attempts to use molecular replacement either with SH2 or SH3 fragments failed. However, the self-rotation function showed the presence of a local twofold axis in the *ab* plane, 18° away from the *a* axis. After screening many heavy-atom derivatives, only one (mercuri-acetate) proved to be useful. This derivative was recorded at 3.1 Å resolution and was used to calculate a SIRAS map that was interpreted with the help of the option Bones of program O (*19*). It was possible to fit two SH2 and four SH3 domains which proved to be related by the previously identified local twofold axis found in the self-rotation. The last features to be traced in the electron density map were the domain junctions. There is only one site for Hg per Grb2 molecule and it corresponds to Cys^{198} of the COOH-terminal SH3. Use of solvent flattening and noncrystallographic symmetry (NCS) included in the Dm program from CCP4 library (*20*) proved to be of the utmost importance. Resolution was gradually increased from 4.5 to 3.1 Å. Graphic reconstruction by program O was done alternately with X-PLOR (*21*) minimization cycles between 7 and 3.1 Å. After each model-building session, transformations were applied from newly built molecule A to molecule B with the matrix calculated by program O. Then B group factors were introduced in the refinement. Tight NCS constraints were maintained during refinement. Annealed omit-maps were used to rebuild several regions. The electron density of loop 28–33 and residue Ser^{141} located in the vicinity of the solvent channel is poorly defined. The crystallographic *R* factor is 21% for all data >2.5σ between 7 and 3.1 Å. No attempt was made to fit water molecules at this stage because of the limited resolution.
13. A. Musacchio, M. Saraste, M. Wilmans, *Nature Struct. Biol.* **1**, 546 (1994); A. Musacchio, M. Noble, R. Pauptit, R. Wierenga, M. Saraste, *Nature* **359**, 851

(1992); M. Noble, A. Musacchio, M. Saraste, S. A. Courtneidge, R. Wierenga, *EMBO J.* **12**, 2617 (1993); T. V. Borchert, M. Matthieu, J. P. Zeelen, S. A. Courtneidge, R. Wierenga, *FEBS Lett.* **341**, 79 (1994).
14. J. Janin, S. Miller, C. Chotia, *J. Mol. Biol.* **204**, 155 (1988).
15. M. J. Eck, S. K. Atwell, S. E. Shoelson, S. C. Harrison, *Nature* **368**, 764 (1994).
16. C. H. Lee *et al.*, *Structure* **2**, 423 (1994).
17. G. Waksman *et al.*, *Nature* **358**, 646 (1992); V. Mikol *et al.*, *J. Mol. Biol.* **246**, 344 (1995).
18. D. Cussac, M. Frech, P. Chardin, *EMBO J.* **13**, 4011 (1994).
19. T. A. Jones *et al.*, *Acta Crystallogr.* **D47**, 110 (1991).
20. Collaborative Computational Project, Number 4, *ibid.* **D50**, 760 (1994).
21. A. T. Brünger, *X-PLOR Version 3.1: A system for X-ray Crystallography and NMR* (Yale Univ. Press, New Haven, CT, 1992).
22. P. J. Kraulis, *J. Appl. Crystallogr.* **24**, 946 (1991).
23. E. A. Merritt, M. P. Murphy, *Acta Crystallogr.* **D50**, 869 (1994).
24. We thank F. Schweighoffer for providing the Grb2 gene construct. We are greatly indebted to R. Fourme and J. P. Benoit for development of the DW32 station and to LURE for express runs. We thank P. Saludjian for help in the use of the AMoRe program, M. Eck and S. Harrison for providing Lck coordinates prior to publication, and B. Tocqué and J. Janin for critical reading of the manuscript. S.M. is supported by MESR and BioAvenir. This project was supported by CNRS and was carried out as part of the BioAvenir program supported by Rhône-Poulenc with the participation of Ministere de l'Enseignement Superieur et de la Recherche and the French Ministry of Industry.

27 January 1995; accepted 2 March 1995

Recruitment and Activation of PTP1C in Negative Regulation of Antigen Receptor Signaling by FcγRIIB1

Daniele D'Ambrosio, Keli L. Hippen, Stacey A. Minskoff, Ira Mellman, Giovanni Pani, Kathy A. Siminovitch, John C. Cambier*

Coligation of the Fc receptor on B cells, FcγRIIB1, with the B cell antigen receptor (BCR) leads to abortive BCR signaling. Here it was shown that the FcγRIIB1 recruits the phosphotyrosine phosphatase PTP1C after BCR coligation. This association is mediated by the binding of a 13–amino acid tyrosine-phosphorylated sequence to the carboxyl-terminal Src homology 2 domain of PTP1C and activates PTP1C. Inhibitory signaling and PTP1C recruitment are dependent on the presence of the tyrosine within the 13–amino acid sequence. Inhibitory signaling mediated by FcγRIIB1 is deficient in *motheaten* mice which do not express functional PTP1C. Thus, PTP1C is an effector of BCR-FcγRIIB1 negative signal cooperativity.

For decades it has been known that immune complexes consisting of antigen and immunoglobulin G (IgG) antibodies are potent inhibitors of humoral immune responses (*1*). Immune complex–mediated inhibition of antibody production has been shown to depend on coligation of BCR and the receptor for the Fc region of IgG (FcγRIIB1) and does not result from independent ligation of the FcγRIIB1 (*2*). Studies indicate that FcγRIIB1 coligation aborts the immune response at the level of BCR signal transduction. BCR signal transduction is mediated by the rapid activation of Src and Syk family tyrosine kinases (*3*), augmented protein tyrosine phosphorylation (*4*), phosphoinositide hydrolysis, and elevation of the cytoplasmic free calcium concentration ($[Ca^{2+}]_i$), which result in B cell proliferation, differentiation, and antibody secretion (*5*). Coligation of BCR and FcγRIIB1 leads to the premature termination of inositol trisphosphate (IP_3) production (*6*), inhibition of the extracellular Ca^{2+} influx (*7*), and blockade of blastogenesis (*8*).

FcγRIIB1 is the only receptor for IgG Fc domains that is detectable on the surface of B lymphocytes (*9*). Mutational analysis of this receptor has revealed that a 13–amino acid motif in the cytoplasmic domain is required for negative signaling (*10*). Muta *et al.* showed that this 13–amino acid sequence mediates inhibitory signaling when it is expressed in an inert receptor context, that phosphorylation of Tyr^{309} in this 13–amino acid "inhibitor" sequence follows BCR coligation, and that this tyrosine is essential for FcγRIIB1-mediated inhibitory signaling (*11*). Although this sequence has only been described in a single receptor, it is operationally termed ITIM (immune receptor tyrosine-based inhibitor motif) in this report. It seemed plausible, given the documentation in many systems of protein phosphotyrosine interaction with SH2 domains (*12*), that this inhibitory signaling might be mediated by FcγRIIB1 recruitment of one or more effectors which bind by means of their SH2 domains to the phosphorylated Tyr^{309} in the ITIM.

To identify such a hypothetical effector we used synthetic nonphosphorylated and tyrosine-phosphorylated (designated by the prefix "p") ITIM peptides with the sequence EAENTIT(p)YSLLKH to isolate binding proteins in lysates of [^{35}S]methionine-labeled A20 cells (*13*). Three proteins, of 160, 70, and 65 kD, bound to pITIM but not to nonphosphorylated ITIM (Fig. 1A). These proteins were purified from 5×10^9 A20 cells by pITIM affinity chromatography and subsequent elution with *p*-nitrophenyl phosphate (*p*NPP is a phosphotyrosine analog), followed by SDS–polyacrylamide gel electrophoresis (PAGE) fractionation and membrane transfer as described (*14*), and subjected to sequence analysis. The NH_2-terminal 17–amino acid sequence of the 65-kD protein was found to be a perfect match for the phosphotyrosine phosphatase PTP1C, also known as HCP, SHP, or SH-PTP1 (*15*). We confirmed the identity of the protein by immunoblotting with antibody to PTP1C (anti-PTP1C) (Fig. 1B). Equal amounts of PTP1C were present in pITIM peptide adsorbates of unstimulated A20 cells, A20 cells stimulated with rabbit antibody against membrane immunoglobulin (mIg), and A20 cells stimulated with $F(ab')_2$ fragments of the antibody (Fig. 1B). This suggests that the association of PTP1C with FcγRIIB1 does not require BCR-induced modification of the enzyme.

To address the physiological relevance of the FcγRIIB1-PTP1C interaction, we determined whether this association occurs in cells. Using the monoclonal antibody 2.4G2 we immunoprecipitated FcγRIIB1 from unstimulated A20 cells and from A20 cells that had been stimulated with intact or $F(ab')_2$ rabbit anti-mIg (*16*). Sequential immunoblotting of SDS-PAGE–fractionated material with anti-FcγRIIB, anti-phosphotyrosine, and anti-PTP1C showed inductive FcγRIIB1 tyrosine phosphorylation (Fig. 1C) and PTP1C co-immunoprecipitation (Fig. 1E) only in cells stimulated with intact anti-mIg. Stimulation had no effect on the amount of FcγRIIB1 immunoprecipitated (Fig. 1D). The stimulation with $F(ab')_2$ anti-mIg did not induce FcγRIIB1 tyrosine phosphorylation or PTP1C association (Fig. 1, C and E). In similar experiments performed with IIA1.6 cells [an FcγRIIB1-negative variant of the A20 cell line (*17*)] neither tyrosine-phosphorylated protein nor PTP1C coprecipitation with the 2.4G2 antibody was detected (*18*). These data demonstrate that BCR-FcγRIIB1 coligation is

D. D'Ambrosio, K. L. Hippen, J. C. Cambier, Division of Basic Sciences, Department of Pediatrics, National Jewish Center for Immunology and Respiratory Medicine, 1400 Jackson Street, Denver, CO 80206, and Department of Microbiology and Immunology, University of Colorado Health Science Center, Denver, CO 80206, USA.
S. A. Minskoff and I. Mellman, Department of Cell Biology, Yale University, School of Medicine, New Haven, CT 06520, USA.
G. Pani and K. A. Siminovitch, Samuel Lunenfeld Research Institute of Mount Sinai Hospital, Toronto, Ontario, Canada, M5G1X5.

*To whom correspondence should be addressed.